JOURNAL OF SOLID STATE CHEMISTRY 82, 279–289 (1989)

Coordination Sites of Metals in Tetrahedrite Minerals Determined by EXAFS

J. M. CHARNOCK AND C. D. GARNER*

Chemistry Department, Manchester University, Manchester M13 9PL, United Kingdom

AND R. A. D. PATTRICK AND D. J. VAUGHAN

Geology Department, Manchester University, Manchester M13 9PL, United Kingdom

Received May 25, 1989

Synchrotron radiation has been used to collect Cu, Ag, Fe, Cd, and Sb K-edge EXAFS data from a series of naturally occurring and synthetic tetrahedrite, $(Cu, Ag)_{10}(Cu, Fe, Zn, Cd)_2Sb_4S_{13}$, minerals. Analysis of the spectra has provided direct evidence about the coordination environment of the various metals, and revealed which sites in the structure each will preferentially occupy. The results complement crystallographic data by giving information about each element in sites occupied by more than one cation, whereas crystallography can only reveal the average geometry of each site. Data from the copper and silver EXAFS have demonstrated that the silver goes into trigonal rather than tetrahedral coordination sites, and in the case of one silver-rich sample a close silver–antimony contact has been identified which provides evidence about the nature of a compression of the structure which is found in this sample. In synthetic samples the iron mainly occupies tetrahedral sites, but in natural tetrahedrites of low silver content, can also go into the trigonal site. The cadmium is tetrahedrally coordinated, and the antimony has threefold tetrahedral geometry with a vacant site, although in the silver-rich sample the antimony–silver interaction is also observed. The results have shown the value of multi-element EXAFS spectroscopy in the investigation of a chemically and structurally complex mineralogical system.

Introduction

Minerals belonging to the tetrahedrite group, represented by the general formula $M^{I}_{10}M^{II}_{2}M^{III}_{4}S_{13}$ (M^{I} = Cu, Ag; M^{II} = Fe, Zn, Cd, Hg, Cu; M^{III} = Sb, As, Bi), have a sphalerite derivative structure of space group $I\bar{4}3m$ (*1–4*), with two unit formulae per unit cell. Figure 1 (*5*) depicts a half-unit cell, with the various coordination sites in $Cu_{12}Sb_4S_{13}$ shown in more detail in Fig. 2. In each half-unit cell ten M^{I} and two M^{II} atoms occupy six fourfold and six threefold coordination sites; the M^{III} atoms occupy the equivalent of a tetrahedral site in sphalerite but are bonded to only three sulfur atoms, resulting in a void in the structure and a lone pair of electrons associated with the M^{III} atoms; 12 S atoms are 4-coordinate and the other single S atom is 6-coordinate.

* To whom correspondence should be addressed.

0022-4596/89 $3.00

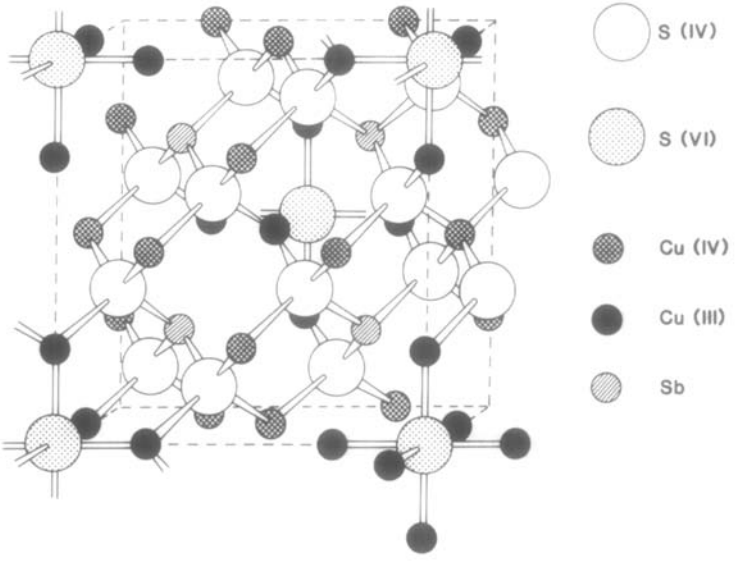

FIG. 1. A half-unit cell of tetrahedrite $Cu_{12}Sb_4S_{13}$ (redrawn from Ref. (*5*)).

Natural and synthetic tetrahedrites are known with a wide range of compositions (*5–9*); samples containing As^{III} rather than Sb^{III} are referred to as tennantites. Commonly in natural samples the two M^{II} atoms are iron and/or zinc, and more rarely mercury and cadmium may also be present. Samples high in copper, tending toward the Cu_{12} end-member, occupy a wide compositional field, which narrows significantly on substitution by these metals (*4, 9*). Tetrahedrites can contain a high proportion of silver by weight and are an important source of this metal. Evidence from crystallographic studies has indicated that in silver-rich tetrahedrites Ag^{I} atoms replace Cu^{I} in trigonal rather than tetrahedral sites (*10–12*). There is disagreement about the coordination site of the M^{II} metal, which has been reported as tetrahedral in Hg- and Fe-containing samples (*11, 13*), but also as trigonal in an Fe-containing sample (*12*). The substitution of different elements also causes changes in cell parameters (*5, 14*) and metal–sulfur distances (*11*). For example, silver substitution for copper causes a systematic increase in cell size in most natural and synthetic tetrahedrites. However, anomalously low cell sizes have been re-

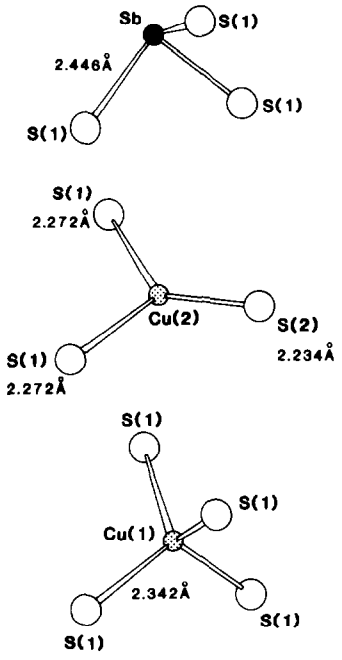

FIG. 2. Coordination polyhedra in tetrahedrite (Ref. (*21*)).

corded in natural Fe-bearing tetrahedrites with silver contents in excess of 4 atoms per half-unit cell (*5*, *15*).

Preliminary EXAFS studies of Cu and Ag spectra support the preferential occupation of trigonal sites by the Ag^{I} atoms (*16*). Combined data from Fe EXAFS and Mössbauer spectroscopy have shown that in natural tetrahedrites the iron mainly occupies tetrahedral sites as Fe^{II}, but that in synthetic samples the oxidation state and coordination changes from Fe^{III} in trigonal sites to Fe^{II} in tetrahedral sites as the degree of silver substitution increases (*17*). We have now extended this work by recording Cu, Ag, Fe, Cd, and Sb EXAFS spectra of a wider range of samples.

Experimental

Samples were finely ground under acetone and pressed into aluminum sample holders with Sellotape windows. The samples were diluted with boron nitride to minimize distortion of the spectra due to the thickness effect (*18*). The EXAFS spectra were recorded in transmission mode at the Daresbury Synchrotron Radiation Source, operating at 2 GeV with an average current of 150 mA: the Cu and Fe spectra were collected at room temperature on stations 7.1 and 8.3, and the Ag, Cd, and Sb spectra at room temperature and/or liquid nitrogen temperature on station 9.2. Double crystal Si(111) (7.1, 8.3) and Si(220) (9.2) monochromators were employed, detuned to reject 50% of the maximum transmitted radiation in order to reduce harmonic contamination. Data analysis utilized the single scattering spherical wave method for calculating EXAFS (*19*), with phase shifts derived from ab initio calculations and refined on model compounds, using the Daresbury program EXCURVE (*20*).

The natural samples (prefixed BM) were provided by the British Museum (Natural History) and are referred to in the IMA/COM data file on ore minerals (*24*). The synthetic tetrahedrites (prefixed RP) were prepared in evacuated silica tubes at 400°C using methods described by Pattrick and Hall (*5*), and mineral analyses performed on a CAMECA CAMEBAX electron microprobe using wavelength spectrometry; standards used were metallic Cu and $CuSbS_2$, FeS_2, $AgBiS_2$, CdS, and ZnS. Compositions of the samples used in this study are given in Table I.

Results and Discussion

Introduction

Analysis of the EXAFS spectra yielded bond lengths, coordination numbers, and Debye–Waller factors, and these are presented in Tables III–VII. The Debye–Waller factors are a measure of the thermal motion of the backscattering atoms with respect to the central absorber, but also depend on the disorder of the system. Thus differences in absorber–scatterer distances in a single site, or a distribution of the absorbing atoms among several sites, will both tend to increase the Debye–Waller factor. The phaseshifts for data interpretation were refined using EXAFS data collected from $CuFeS_2$ (chalcopyrite), CdS (greenockite), and Ag_3SbS_3 (pyrargyrite). For chalcopyrite these calibrated phaseshifts gave coordination numbers and bond lengths of 3.9 S atoms at 2.252 Å and 3.9 S atoms at 2.298 Å for the Cu and Fe, respectively, having calibrated using 4 S atoms at 2.257(1) Å and 4 S atoms at 2.302(1) Å derived from X-ray crystallographic results (*21*). In greenockite the EXAFS analysis yielded 3.8 S atoms at 2.517 Å, compared with 4 S atoms at 2.52 Å in the crystal structure (*22*) (error not quoted). In pyrargyrite the Ag EXAFS gave 1.9 S atoms at 2.447 Å, with crystallography showing 1 S atom at 2.43(2) Å and 1 S atom at 2.45(0) Å, and the Sb spectrum gave 3 S atoms at 2.454 Å,

TABLE 1

CHEMICAL COMPOSITIONS OF THE SAMPLES USED IN THIS STUDY

Sample[a]	Composition (wt%)								Total	Formula[b]
	Cu	Ag	Fe	Zn	Cd	As	Sb	S		
BM15480	47.5		4.3			20.1		28.4	100.3	$Cu_{10.9}Fe_{1.1}As_{3.9}S_{12.9}$
BM88670	38.0		1.3	6.3		0.7	28.9	24.4	99.6	$Cu_{10.0}Fe_{0.4}Zn_{1.6}As_{0.2}Sb_{4.0}S_{12.7}$
BM1929,64	37.7	0.4	5.5	1.8		0.8	29.3	24.9	100.4	$Cu_{9.9}Ag_{0.1}Fe_{1.6}Zn_{0.5}As_{0.2}Sb_{4.0}S_{12.9}$
BM40456	33.8	7.0	1.0	6.4		1.9	26.6	24.1	100.8	$Cu_{9.0}Ag_{1.1}Fe_{0.3}Zn_{1.7}As_{0.4}Sb_{3.7}S_{12.7}$
BM57605	27.3	15.1	3.6	3.3		0.9	27.3	23.2	100.7	$Cu_{7.5}Ag_{2.4}Fe_{1.2}Zn_{0.9}As_{0.2}Sb_{3.9}S_{12.7}$
BM88668	15.3	31.7	5.0	1.0		0.2	26.6	20.5	100.3	$Cu_{4.5}Ag_{5.5}Fe_{1.7}Zn_{0.3}As_{0.1}Sb_{4.1}S_{12.5}$
RP25B	42.8		3.3				29.6	25.0	100.7	$Cu_{11.0}Fe_{1.0}Sb_{4.0}S_{12.8}$
RP17A	38.0	4.5	3.1				29.0	24.2	98.8	$Cu_{10.3}Ag_{0.7}Fe_{1.0}Sb_{4.1}S_{13.0}$
RP17B	31.9	12.5	3.4				27.9	23.3	99.0	$Cu_{8.9}Ag_{2.1}Fe_{1.1}Sb_{4.0}S_{12.8}$
RP11B	25.1	18.8	4.7				28.0	22.2	98.8	$Cu_{7.3}Ag_{3.2}Fe_{1.6}Sb_{4.2}S_{12.6}$
RP11D	13.9	34.1	5.8				26.6	20.9	101.3	$Cu_{4.1}Ag_{5.9}Fe_{2.0}Sb_{4.2}S_{12.5}$
RP1D	29.0	7.7			12.7		27.4	22.3	99.1	$Cu_{8.6}Ag_{1.3}Cd_{2.1}Sb_{4.2}S_{13.1}$
RP1C	22.1	18.8			11.5		25.9	21.0	99.3	$Cu_{6.7}Ag_{3.4}Cd_{1.9}Sb_{4.0}S_{12.6}$
RP14C	9.8	35.1			11.2		25.2	19.2	100.5	$Cu_{3.2}Ag_{6.7}Cd_{2.1}Sb_{4.3}S_{12.4}$

[a] Prefix BM denotes natural sample, and RP synthetic.

[b] Calculated for total $M^{I} + M^{II} = 12$.

with the crystal structure giving 3 S atoms at 2.45(1) Å (*23*). Therefore we have quoted errors for parameters derived from EXAFS data of ±0.5 for the absolute value of the coordination number and ±0.01 Å for the absolute value of the bond length in the first shell, with greater uncertainty in outer shells. Changes in these parameters are easily distinguished by direct comparisons. For example, the Fourier transforms of the Cu EXAFS spectra of BM88670, BM40456, and BM88668 in Fig. 3 show clear differences in respect of the shift to higher R value of the major peak in the Fourier transform, and the increase in the amplitude of this peak along the series. The Cu–S bond lengths obtained from the interpretation of the EXAFS data are 2.276, 2.294, and 2.313 Å, respectively, and the corresponding coordination numbers were determined as 3.4, 3.5, and 4.1.

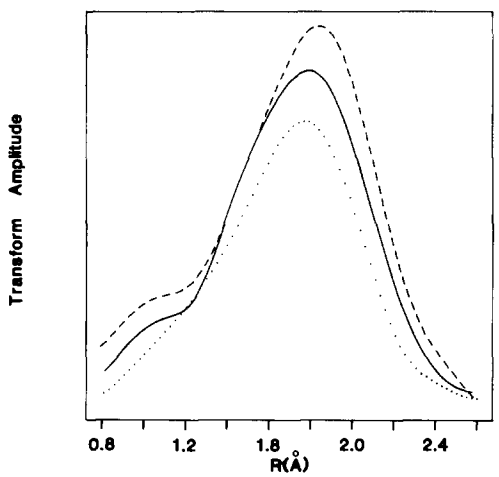

FIG. 3. Fourier transforms of the Cu EXAFS spectra of BM88670 (. . .), BM40456 (—), and BM88668 (– – –).

The near edge regions of the absorption spectra (XANES), extending from about 20 eV below to 50 eV above the edge, in most cases showed the pre-edge feature usually associated with noncentrosymmetric coordination sites, but no obvious changes were observed on substitution which would distinguish between the trigonal and tetrahedral sites (*16*), so these will not be discussed further.

TABLE II

BOND LENGTHS (Å) FROM STRUCTURAL REFINEMENTS OF TETRAHEDRITES (*2, 10–12*)

Atom pair	Silver content[a]				
	Ag_0^2	$Ag_{0.1}^{12}$	$Ag_{2.1}^{11}$	$Ag_{2.2}^{10}$	$Ag_{4.2}^{12}$
Cu(IV)–S(IV)	2.342	2.332	2.34	2.336	2.340
Cu(III)–S(IV)	2.270	2.274	2.43	2.360	2.429
Cu(III)–S(VI)	2.234	2.229	2.27	2.278	2.299
Sb(III)–S(IV)	2.446	2.432[b]	2.39[c]	2.435	2.448
Cu(III)–Sb(lone pair)	3.000		3.04	3.047	

[a] Atoms per unit formula.
[b] Contains 0.3 atoms As.
[c] Contains 1.3 atoms As.

The samples fall into three groups comprising natural, iron-containing, and cadmium-containing synthetic samples (Table I). The silver contents of the natural samples range from 0 to 5.5 atoms per half-unit cell and they have variable Zn : Fe (M^{II}) ratios. Of particular interest are the data from sample BM88668 which is a silver-rich tetrahedrite with an anomalously low (collapsed) cell size. The iron- and cadmium-containing synthetic samples also have a wide range of silver contents, and two of these, RP11D and RP14C, have greater than 4 silver atoms per half-unit cell but do not have anomalously low cell sizes.

Structural refinement data have been recorded by several groups for tetrahedrites with variable silver content and this information is summarized in Table II. The metal–sulfur distances in this table represent average values for a particular site irrespective of which element occupies that site, in contrast to the bond lengths derived from EXAFS which are averages for a particular element irrespective of site. This means that the crystallographic and EXAFS data relating to elements in the two Cu sites (i.e., the trigonal or M(III) site and the tetrahedral or M(IV) site) may not be directly comparable, although comparison is still useful and the information is sometimes complementary.

Copper

The Cu EXAFS spectra could all be fitted using a single shell of sulfur atoms around the central copper, with very little contribution from further shells; this is is illustrated in Fig. 4 for sample BM15480, showing the excellent agreement between the theoretically generated spectrum and the experimental data, together with their associated Fourier transforms. Analysis of the data yielded the parameters displayed in Table III, which also includes previously published data (*16*). These represent averages of the contributions from the copper atoms in each of the possible sites, M(III) and M(IV), and changes in the parameters reflect changes in the distribution of copper between them. Thus, as a longer bond

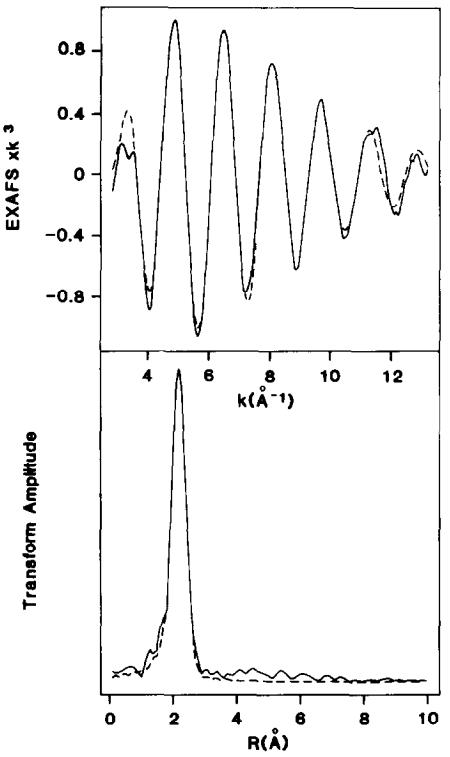

FIG. 4. The k^3-weighted Cu EXAFS spectrum (solid line, top) and Fourier transform (solid line, bottom) of BM15480. The broken lines represent the best-fit theoretical simulation.

TABLE III

PARAMETERS DERIVED FROM THE COPPER EXAFS SPECTRA

Sample	Cu : Ag	R(Å)[a]	N[b]	$2\sigma^2$(Å^2)[c]
RP25B	11.0 : 0.0	2.279	3.4	0.018
RP17A	10.3 : 0.7	2.284	3.6	0.019
RP17B	8.9 : 2.1	2.295	3.6	0.018
RP11B	7.3 : 3.2	2.298	3.7	0.020
RP11D	4.1 : 5.9	2.302	3.8	0.020
RP1D[d]	8.6 : 1.3	2.286	3.5	0.017
RP1C	6.7 : 3.4	2.291	3.7	0.020
RP14C	3.2 : 6.7	2.299	3.8	0.021
BM15480	11.0 : 0.0	2.277	3.4	0.022
BM88670	10.0 : 0.0	2.276	3.4	0.019
BM1929,64	9.9 : 0.1	2.282	3.5	0.020
BM40456[d]	9.0 : 1.1	2.294	3.5	0.019
BM57605[d]	7.5 : 2.4	2.302	3.7	0.018
BM88668[d]	4.5 : 5.5	2.318	4.1	0.017

[a] Average Cu–S bond length in first coordination shell ±0.01 Å.

[b] Average coordination number ±0.5.

[c] Debye–Waller factor.

[d] Published in Ref. (*16*).

length and higher coordination number are associated with the tetrahedral M(IV) site (Fig. 2), an increase in these parameters would imply a greater relative occupation by copper of this site. Coordination numbers range from 3.4 in silver-free tetrahedrites to 4.1 in highly argentiferous samples, and the bond lengths range from 2.278 to 2.318 Å; these changes are clearly reflected in the Fourier transforms in Fig. 3, in which the peak position and amplitude both increase as the silver content increases. Analysis of the data shows a systematic increase of coordination number and bond length with increasing silver content, which demonstrates the preferential displacement of copper by silver from the M(III) sites.

The Cu–S distance of ca. 2.28 Å for silver-free tetrahedrites (Table III) is close to the expected value intermediate between the Cu(IV)–S and Cu(III)–S bond lengths derived from crystallographic data (Table II). In the highest silver synthetic tetrahedrites (RP14C and RP11D) all the M(III) sites are potentially occupied by Ag, and therefore Cu could exclusively occupy the M(IV) sites. However, the Cu–S distance of 2.30 Å is significantly lower than the average M(IV)–S value of 2.34 Å from crystallographic data. Since the crystallographic refinements did not resolve the contribution of different elements in particular sites, Fe(IV)–S (and possibly Ag(IV)–S) would have contributed to the M(IV)–S distances shown in Table II. Therefore the discrepancy between the EXAFS and crystallographic values for the Cu–S distance can be explained by the smaller covalent radius of Cu^{I} (0.635 Å) as compared to Fe^{II} (0.660 Å) in the tetrahedral sites, but we cannot exclude the possibility that some copper is still present in the M(III) sites in these samples. However, the Cu EXAFS data of sample BM88668 reveals this sample to have the highest coordination number (4.1) and Cu–S bond length (2.318 Å) of all the tetrahedrites studied, suggesting the copper to be predominantly in the M(IV) site.

Silver

The parameters derived from the room temperature Ag spectra are listed in Table IV, together with previously published data from two samples run at liquid nitrogen temperature (*16*). With the exception of BM88668 the spectra could all be fitted with a single shell of sulfur backscatterers around the silver, with bond lengths and coordination numbers independent of the sample composition. These results indicate that the silver occupies the same site in each sample, and the average coordination number of 3.0 adds further confirmation that this is the M(III) site rather than the M(IV) site. The average Ag–S bond length in the EXAFS analyses of 2.52 Å represents the Ag(III)–S distance in tetrahe-

TABLE IV

PARAMETERS DERIVED FROM ROOM TEMPERATURE SILVER EXAFS SPECTRA

Sample	Cu : Ag	Scatterer	R(Å)[a]	N[b]	$2\sigma^2$(Å^2)[c]
RP11B	7.3 : 3.2	S	2.518	2.9	0.018
RP1D	8.5 : 1.3	S	2.520	2.9	0.017
RP1C	6.7 : 3.3	S	2.518	3.0	0.016
RP14C	3.2 : 6.7	S	2.515	3.1	0.017
BM40456	9.0 : 1.1	S	2.513	3.1	0.016
BM57605	7.5 : 2.4	S	2.520	3.0	0.017
BM57605[d]		S	2.514	2.8	0.017
BM88668	4.5 : 5.5	S	2.549	2.2	0.019
		Sb	2.796	1.5	0.020
BM88668[d]		S	2.555	1.7	0.018
		Sb	2.888	1.6	0.007

[a] Average Ag-scatterer distance ±0.01 Å (first shell), ±0.05 Å (second shell).

[b] Average coordination number ±0.5.

[c] Debye–Waller factor.

[d] Low temperature (−196°) data from Ref. (*16*), analyzed using uncalibrated phaseshifts.

drites, and the replacement of Cu by the considerably larger Ag explains the increase in the M(III)–S distances observed in the structural refinements of argentian tetrahedrites (Table II).

The room temperature Ag EXAFS spectrum from sample BM88668 contrasts with the other Ag data, clearly showing contributions from two shells, illustrated in Fig. 5, as has also been reported for data collected previously at −196°C (*16*). A good fit was obtained using a shell of sulfurs at 2.549 Å and a shell of antimonies at 2.796 Å around the silver. The interference between the EXAFS oscillations from these shells makes assignment of coordination numbers subject to much greater error than in single shell spectra, so that the low sulfur coordination number found for this sample is not necessarily a true reflection of the actual bonding. However, the bond length determination is no less accurate than that for the other samples, so the slight increase in the Ag–S bond length from ca. 2.52 to 2.55 Å may represent a real difference. More importantly, the presence of the second shell in this spectrum is a clear indication that the silver is in a different environment in this sample with a collapsed unit cell as compared to the other tetrahedrites, and it is reasonable to assume that the Ag–Sb interaction is related to the collapse. This is dealt with more fully in the discussion section.

Iron

Much of the data from the Fe EXAFS (Table V) has been presented and discussed previously in combination with Fe Mössbauer measurements (*17*). These results are included for completeness, and to allow discussion and comparison with the other

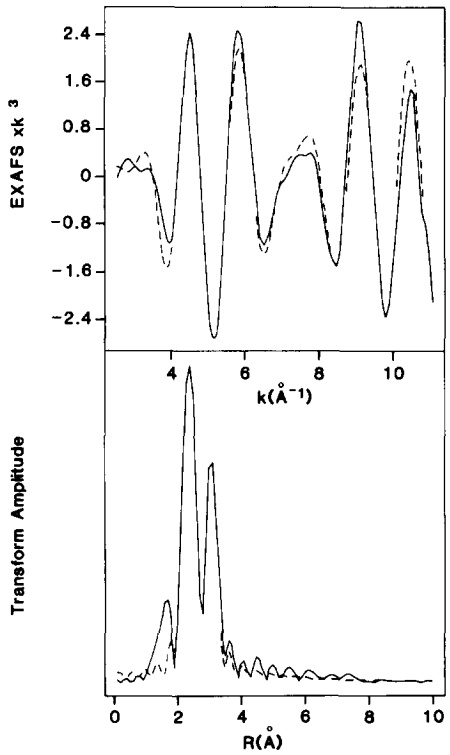

FIG. 5. The k^3-weighted Ag EXAFS spectrum (solid line, top) and Fourier transform (solid line, bottom) of BM88668. The broken lines represent the best-fit theoretical simulation.

TABLE V

PARAMETERS DERIVED FROM IRON EXAFS SPECTRA (PREVIOUSLY PUBLISHED IN REFERENCE (*17*), EXCEPT BM1929,64)

Sample	Cu : Ag : Fe	R(Å)[a]	N[b]	$2\sigma^2$(Å^2)[c]
RP25B	11.0 : 0.0 : 1.0	2.268	3.0	0.002
RP17A	10.3 : 0.7 : 1.0	2.275	3.2	0.002
RP17B	8.9 : 2.0 : 1.1	2.283	3.3	0.006
RP11B	7.3 : 3.2 : 1.5	2.290	3.7	0.012
RP11D	4.1 : 5.9 : 2.0	2.307	3.9	0.016
BM15480	11.0 : 0.0 : 1.0	2.307	4.0	0.012
BM88670	10.0 : 0.0 : 0.4	2.301	3.7	0.014
BM1929,64	9.9 : 0.1 : 1.6	2.300	3.8	0.016
BM40456	9.0 : 1.1 : 0.3	2.300	3.7	0.011
BM57605	7.5 : 2.4 : 1.2	2.313	3.8	0.010
BM88668	4.5 : 5.5 : 1.8	2.301	3.7	0.012

[a] Average Fe–S bond length in first coordination shell ±0.01 Å.
[b] Average coordination number ±0.5.
[c] Debye–Waller factor.

EXAFS data. The additional spectrum (BM88670) fits into the pattern already established (*17*) which showed that the iron in natural samples tends to occupy tetrahedral sites, but in synthetic samples may occupy trigonal sites as Fe^{III} when the silver concentration is low, and is displaced into tetrahedral sites as Fe^{II} as the silver content increases.

Cadmium

Each of the three Cd spectra analyzed in Table VI could be fitted by a single shell of four sulfur atoms at 2.48 Å, and showed no dependence on the silver concentration. These bond lengths and coordination numbers are consistent with tetrahedral coordination (*22*).

Antimony

Analysis of the Sb spectra yielded the result that in all samples the antimony atoms were coordinated to three sulfurs, with a bond length of 2.43 Å which is insensitive to silver substitution (Table VII). These

TABLE VI

PARAMETERS DERIVED FROM CADMIUM EXAFS SPECTRA

Sample	Cu : Ag : Fe	R(Å)[a]	N[b]	$2\sigma^2$(Å^2)[c]
RP1D	8.5 : 1.3 : 2.1	2.483	4.0	0.013
RP1C	6.7 : 3.3 : 1.9	2.482	3.9	0.012
RP14C	3.2 : 6.7 : 2.1	2.479	3.7	0.012

[a] Average Cd–S bond length in first coordination shell ±0.01 Å.
[b] Average coordination number ±0.5.
[c] Debye–Waller factor.

values are in good agreement with the Sb–S distances derived from crystallographic data (Table II). The room temperature spectrum of sample BM88668, for which the silver spectrum had shown a silver–antimony interaction, showed only a single shell of sulfur backscatterers. However, a spectrum recorded at −196°C revealed further shells, including the antimony–silver contact at 2.83 Å, and a shell of sulfur atoms at 3.50 Å (Fig. 6). The Sb–Ag distance of 2.83 Å agrees within the experimental

TABLE VII

PARAMETERS DERIVED FROM ANTIMONY EXAFS SPECTRA, RECORDED AT ROOM TEMPERATURE EXCEPT WHERE INDICATED

Sample	Scatterer	R(Å)[a]	N[b]	$2\sigma^2$(Å^2)[c]
RP11B	S	2.433	2.7	0.009
RP1D	S	2.427	3.0	0.009
RP1C	S	2.430	3.1	0.009
RP14C	S	2.424	3.0	0.010
BM40456	S	2.427	3.0	0.009
BM57605	S	2.432	2.9	0.008
BM88668	S	2.426	3.0	0.009
BM88668[d]	S	2.419	2.8	0.006
	Ag	2.834	0.9	0.009
	S	3.500	4.4	0.023

[a] Average Sb-scatterer distance ±0.01 Å (first shell), ±0.05 Å (outer shells).
[b] Average coordination number ±0.5.
[c] Debye–Waller factor.
[d] Spectrum recorded at −196°C.

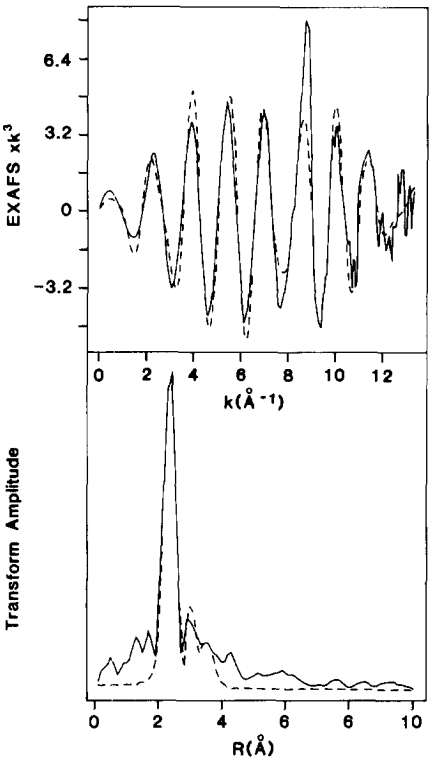

FIG. 6. The k^3-weighted Sb EXAFS spectrum (solid line, top) and Fourier transform (solid line, bottom) of BM88668, recorded at −196°C. The broken lines represent the best-fit theoretical simulation.

error with that of 2.80 Å found in the silver spectrum. The failure to observe the second shell in the room temperature spectrum was probably due to the increase in the Debye–Waller factor from 0.007 to 0.020 Å^2 on warming (Table VI), which would cause a decrease in the contribution of this shell to the total EXAFS. Furthermore, the lower Debye–Waller factor in the first (*M*–S) shell of the antimony spectrum compared to that of the silver spectrum leads to a greater relative contribution of that shell to the antimony EXAFS, which is clearly seen in the difference between Figs. 5 and 6.

Discussion

The EXAFS parameters from the Cu and Ag spectra clearly demonstrate the preferential substitution of copper in the trigonal site by silver. The consistent Ag–S bond length in the synthetic tetrahedrites could be interpreted as being a result of the random distribution of silver between the two possible sites, as has been suggested (*12*), but the trends observed in the Cu EXAFS of the same samples show that this is not the case. The data cannot entirely preclude the incorporation of some silver into the tetrahedral site, and indeed there must be some Ag(IV) present in sample RP14C. However, there is little evidence from either the Cu or the Ag spectra of sample BM88668 that Ag(IV) is present, and therefore no support for the suggestion that a switch from substitution of Ag(III) to Ag(IV) causes the cell size collapse. The Fe and Cu EXAFS data from the synthetic samples display parallel trends of increasing *R* and *N* values as Cu(III) is replaced and Fe(III) is displaced by silver. By combining the EXAFS and Mössbauer data the substitutional series can be described as

$$6Cu^{I}(IV) \cdot 5Cu^{I}(III) \cdot Fe^{III}(III) \Leftrightarrow 4Cu^{I}(IV) \cdot 6Ag^{I}(III) \cdot 2Fe^{II}(IV) \quad (17).$$

The bond length changes observed in the Cu and Fe data are explained by changes in the distributions of the metals between two sites, and it can be seen that the bond lengths of the elements that occupy a single site, Cd and Sb, are unaffected by silver substitution. Therefore, the cell size changes observed on substitution (i.e., expansion of the cell parameter) are probably due to the longer silver–sulfur bonds causing changes in bond angles and rotation of polyhedra (*11*) rather than stretching of other metal–sulfur bonds. In the end-member tetrahedrite $Cu_{12}Sb_4S_{13}$ the Sb forms three short bonds to S(IV) atoms, directed toward the corners of a tetrahedron with a vacant site at the fourth vertex, and the distance between the Sb and S(VI) site is 4.033 Å, equal to the sum of the van der Waals radii of antimony and sulfur (*2*). In tennan-

tite ($Cu_{12}As_4S_{13}$) the As–S(VI) distance is 4.057 Å which is greater than the sum of the arsenic and sulfur van der Waals radii (*3*). Wuensch *et al.* (*3*) pointed out that the greater Cu(III)–S length in tetrahedrite causes the Cu(IV) tetrahedron to rotate, but that van der Waals forces between the Sb and S(VI) atoms prevent further distortion. A crystal structure refinement of an argentian tetrahedrite shows the Cu(IV) tetrahedron more regular but rotated further, and the Sb–S(VI) distance remains the same (*11*). If further substitution of copper by silver occurs, the rotation can only continue if the van der Waals forces are overcome and the Sb moves closer to the S(VI) site. This will bring the Sb into contact with the *M*(III) site, which would explain the second shells in the Ag and Sb EXAFS spectra of BM88668, and would also provide a reasonable mechanism for the cell size collapse in this sample. The cell size collapse seen in most natural high silver content tetrahedrites has not been found in synthetic samples of similar compositions (*5, 21*); this may be due to the presence of a small amount of Ag in the *M*(IV) sites preventing rotation of the tetrahedron, as the high temperature required for synthesis would favor a more even distribution of the metals in each site.

Conclusion

This study has shown how EXAFS spectroscopy may be used to provide element-specific information about coordination sites in a relatively complex mixed-metal system. By comparing a series of closely related samples it has proved possible to show the effect of substitution on the distribution of various metals between two different coordination sites, whereas the large errors associated with assignment of coordination numbers from EXAFS data would not generally have allowed unambiguous identification of the coordination site of a metal from only one spectrum. In similar systems where data are available there is a good agreement between EXAFS parameters and those measured by crystallography, which adds support to the conclusions reached by EXAFS about the other samples. The EXAFS and crystallographic data are complementary in that EXAFS provides information about each element in sites occupied by more than one cation, for example, silver in the *M*(III) sites, whereas crystallography can only reveal the average geometry of each site. The information gained by the systematic collection of data at different edges in the same samples gives a clear picture of how the various metal sites change on substitution, and has shown the effect of the cell size collapse in BM88668 on each site. The Ag–Sb interaction, seen clearly in the Ag spectrum and also observed in the low temperature Sb spectrum, provides an explanation for this collapse.

Acknowledgments

We are grateful to the SERC for financial support and the Director of Daresbury Laboratory for provision of facilities. We also thank Drs. S. S. Hasnain and G. P. Diakun for technical assistance. The samples of natural tetrahedrite were provided by Dr. C. J. Stanley of the British Museum (Natural History).

References

1. L. Pauling and E. W. Neumann, *Z. Kristallogr.* **88,** 54 (1934).
2. B. J. Wuensch, *Z. Kristallogr.* **119,** 437 (1964).
3. B. J. Wuensch, Y. Takeuchi, and W. Nowacki, *Z. Kristallogr.* **123,** 1 (1966).
4. E. Makovicky and B. J. Skinner, *Canad. Mineral.* **17,** 619 (1979).
5. R. A. D. Pattrick and A. J. Hall, *Mineral. Mag.* **47,** 441 (1983).
6. M. Charlat and C. Levy, *Bull. Soc. Fr. Mineral. Cristallogr.* **97,** 241 (1974).
7. R. A. D. Pattrick, Ph.D. thesis, University of Strathclyde (1981).

8. N. E. JOHNSON, J. R. CRAIG, AND J. D. RIMSTIDT, *Canad. Mineral.* **24,** 385 (1986).
9. K. TATSUKA AND N. MORIMOTO, *Amer. Mineral.* **58,** 425 (1973).
10. R. KALBSKOPF, *Tschermaks Mineral. Petrogr. Mitt.* **18,** 147 (1972).
11. M. L. JOHNSON AND C. W. BURNHAM, *Amer. Mineral.* **70,** 165 (1985).
12. R. C. PETERSEN AND I. MILLER, *Mineral. Mag.* **50,** 717 (1986).
13. R. KALBSKOPF, *Tschermaks Mineral. Petrogr. Mitt.* **16,** 173 (1971).
14. M. CHARLAT AND C. LEVY, *Bull. Soc. Fr. Mineral. Cristallogr.* **98,** 152 (1975).
15. J. F. RILEY, *Mineral. Deposita* **9,** 117 (1974).
16. J. M. CHARNOCK, C. D. GARNER, R. A. D. PATTRICK, AND D. J. VAUGHAN, *Phys. Chem. Minerals* **15,** 296 (1988).
17. J. M. CHARNOCK, C. D. GARNER, R. A. D. PATTRICK, AND D. J. VAUGHAN, *Mineral. Mag.* **53,** 193 (1989).
18. E. A. STERN AND K. KIM, *Phys. Rev. B* **23,** 3781 (1981).
19. P. A. LEE AND J. B. PENDRY, *Phys. Rev. B* **11,** 2795 (1975).
20. S. J. GURMAN, N. BINSTEAD, AND I. ROSS, *J. Phys. C* **17,** 143 (1984).
21. S. R. HALL AND J. M. STEWART, *Acta Crystallogr. B* **29,** 579 (1973).
22. F. ULRICH AND W. H. ZACHARIASEN, *Z. Kristallogr.* **62,** 260 (1925).
23. P. ENGEL AND W. NOWACKI, *N. Jahrb. Mineral. Monat.,* 181 (1966).
24. A. J. CRIDDLE AND C. J. STANLEY (Eds.), "Commission on Ore Microscopy; IMA/COM Quantitative Data File for Ore Minerals, 2nd issue, British Museum (Natural History) (1986).